

# Design of *Escherichia coli*-Expressed Stalk Domain Immunogens of H1N1 Hemagglutinin That Protect Mice from Lethal Challenge

Gayathri Bommakanti,<sup>a\*</sup> Xianghan Lu,<sup>b</sup> Michael P. Citron,<sup>b</sup> Tariq Ahmad Najar,<sup>a</sup> Gwendolyn J. Heidecker,<sup>b</sup> Jan ter Meulen,<sup>b</sup> Raghavan Varadarajan,<sup>a,c</sup> and Xiaoping Liang<sup>b</sup>

Molecular Biophysics Unit, Indian Institute of Science, Bangalore, India<sup>a</sup>; Merck Research Laboratories, West Point, Pennsylvania, USA<sup>b</sup>; and Chemical Biology Unit, Jawaharlal Nehru Centre for Advanced Scientific Research, Jakkur, Bangalore, India<sup>c</sup>

The hemagglutinin protein (HA) on the surface of influenza virus is essential for viral entry into the host cells. The HA1 subunit of HA is also the primary target for neutralizing antibodies. The HA2 subunit is less exposed on the virion surface and more conserved than HA1. We have previously designed an HA2-based immunogen derived from the sequence of the H3N2 A/HK/68 virus. In the present study, we report the design of an HA2-based immunogen from the H1N1 subtype (PR/8/34). This immunogen (H1HA0HA6) and its circular permutant (H1HA6) were well folded and provided complete protection against homologous viral challenge. Antisera of immunized mice showed cross-reactivity with HA proteins of different strains and subtypes. Although no neutralization was observable in a conventional neutralization assay, sera of immunized guinea pigs competed with a broadly neutralizing antibody, CR6261, for binding to recombinant Viet/04 HA protein, suggesting that CR6261-like antibodies were elicited by the immunogens. Stem domain immunogens from a seasonal H1N1 strain (A/NC/20/99) and a recent pandemic strain (A/Cal/07/09) provided cross-protection against A/PR/8/34 viral challenge. HA2-containing stem domain immunogens therefore have the potential to provide subtype-specific protection.

Influenza virus, the causative agent of flu, is responsible for yearly epidemics and frequent pandemics around the world. The virus changes its genetic makeup constantly to escape the immune pressure from the host, causing fresh epidemics. The envelope of the virus has two major glycoproteins: hemagglutinin (HA) and neuraminidase (NA). HA is a trimer of HA1 and HA2 dimers that are produced by cleavage of the precursor HA0. The globular head domain of the protein is composed exclusively of HA1 and is involved in binding of the virus to host cell sialic acid receptors leading to endosomal uptake of the virus into the cell. HA2, along with regions of HA1, forms the membrane-proximal stalk that is in a metastable conformation, poised to change its conformation upon exposure to the low pH of the endosomes. This conformational change brings about fusion of viral and host endosomal membranes and release of the viral contents into the cytoplasm (25).

Antibodies (Abs) generated against the HA glycoprotein are responsible for conferring protection against viral infection (12). The antibodies generated against the HA protein during natural infection are primarily directed against the exposed head domain (35). Mutations or recombination events involving the HA and NA genes lead to genetic drift and shift, giving rise to new viruses that are not susceptible to previously acquired immunity by the host. In order to be effective, vaccines have to match the currently circulating viral strains, necessitating the production of new vaccines every season. Therefore, the search for a universal vaccine that provides broader protection and alleviates the need for frequent vaccination is ongoing.

A sequence analysis of the HA sequences from various strains and subtypes reveals that HA2 is more conserved than the HA1 subunit (2, 19). However, the immune response primarily targets the globular head domain (HA1), and HA2-directed antibodies were not thought to contribute to neutralization of the virus (35). In the recent past, several broadly neutralizing antibodies that are directed against conserved epitopes in the stalk region of HA have

also been isolated (8, 20, 30, 34). These antibodies are capable of binding not only several strains of viruses within the same HA subtype but also strains of other subtypes belonging to the same clade. These antibodies have been shown to have neutralizing activity and provide cross-strain protection in animal models (21, 26). Monoclonal antibodies directed to the fusion peptide of HA2 have been shown to react with several subtypes of viruses (29). An immunogen that focuses the immune response to the HA2 fragment and elicits Abs against conserved stem epitopes might therefore confer protection against multiple strains of the virus.

Although it is desirable to use the HA2 fragment as an immunogen, expressing HA2 in the absence of HA1 in *Escherichia coli* results in a protein that adopts the low-pH conformation (5). We have earlier shown that by retaining interacting HA1 residues and introducing mutations that destabilize the low-pH conformation of the molecule, it is possible to design a stable immunogen comprising the HA2 subunit of the A/HK/68 virus from the H3N2 subtype (2). Following up on this work, we have now designed immunogens H1HA0HA6\_PR8 and a circular permutant H1HA6\_PR8 from the influenza A/PR/8/34 virus (an H1N1 virus). These proteins, when recombinantly expressed in *E. coli*, purified, and used as immunogens, provided protection against a lethal homologous virus challenge. Sera from immunized animals cross-reacted with recombinant HA proteins from several strains

Received 12 June 2012 Accepted 22 September 2012

Published ahead of print 26 September 2012

Address correspondence to Raghavan Varadarajan, varadar@mbu.iisc.ernet.in, or Xiaoping Liang, xiaoping\_liang@merck.com.

\* Present address: Gayathri Bommakanti, Emory Vaccine Center, Atlanta, Georgia, USA.

Copyright © 2012, American Society for Microbiology. All Rights Reserved.

doi:10.1128/JVI.01429-12

and subtypes of HA. Antisera from immunized guinea pigs competed with a broadly neutralizing antibody, CR6261, showing that the immunogens were capable of eliciting antibodies against the conserved CR6261 epitope of the HA stalk. Stem domain immunogens from both a drifted seasonal flu strain (A/NC/20/99) and a recent pandemic flu strain (A/Cal/07/09) protected immunized mice from a lethal A/PR/8/34 viral challenge. This suggests that HA2-based immunogens can provide cross-protection against several strains within a subtype and play an important role in pandemic preparedness.

## MATERIALS AND METHODS

**Modeling the low-pH form of HA2 fragment residues 51 to 103 from A/PR/8/34.** The trimeric structure of the region of residues 51 to 103 of HA2 from the PR/8/34 strain was modeled using the program Modeler 9v4 (9, 24). The corresponding fragments from the low-pH structure of HK/68 HA (Protein Data Bank [PDB] ID 1htm) were used as the template for the homology modeling.

**Cloning, expression, and purification of the proteins.** *E. coli* codon optimized genes for H1HA6\_PR8 and H1HA0HA6\_PR8 were synthesized. The genes for H1HA6\_PR8, H1HA6\_NC99, and H1HA6\_Cal09 were cloned into pET-26b(+) between NdeI and HindIII sites. The H1HA0HA6\_PR8 gene was cloned into pET-28a(+) between NdeI and BamHI sites. Cloning resulted in addition of a 6-His tag in all the constructs. BL21(DE3) cells transformed with the plasmids were grown in 2 liters Terrific broth to an  $A_{600}$  of 0.8 at 37°C and induced with 1 mM IPTG (isopropyl- $\beta$ -D-thiogalactopyranoside). The cells were harvested after 6 h of induction and lysed by sonication in 20 mM Tris (pH 8.0). The cell lysate was centrifuged at  $18,500 \times g$ , 4°C. The pellet was washed with 0.05% Triton X-100 in 20 mM Tris (pH 8.0) followed by centrifugation at  $18,500 \times g$ , 4°C. The pellet was solubilized using 8 M guanidine hydrochloride (GdnHCl) in 20 mM Tris (pH 8.0). Solubilized and clarified inclusion bodies were passed over an Ni-NTA column (GE Health Care) at room temperature (RT) and eluted in 1 M GdnHCl, 500 mM imidazole, 20 mM Tris (pH 8.0). The proteins were then refolded by dialysis against deionized water and stored at  $-80^\circ\text{C}$ .

**CD spectroscopy.** All spectra were acquired at 298 K. The circular dichroism (CD) spectra of the proteins at a concentration of 5  $\mu\text{M}$  were recorded in  $1 \times$  phosphate-buffered saline (PBS) on a JASCO J-715 Spectropolarimeter. The spectra were recorded using a 0.1-cm-path-length cuvette by scanning from 250 nm to 195 nm at a rate of 50 nm/min with a spectral bandwidth of 2 nm, response time of 4 s, and scan rate of 50 nm/min. Each spectrum is an average of 3 scans and is subtracted for buffer control. Mean residue ellipticities (MRE) were calculated as described previously (18).

**Fluorescence spectroscopy.** The intrinsic fluorescence emission spectrum of the proteins at a concentration of 2  $\mu\text{M}$  was recorded using a 1-cm-path-length cuvette under native (20 mM Tris, pH 8.0) or denaturing conditions (6 M GdnHCl, 20 mM Tris, pH 8.0) after excitation at 280 nm on a Fluoromax-3 fluorimeter. The emission spectra were recorded between 300 and 400 nm at 25°C using excitation and emission bandwidths of 3 nm and 5 nm, respectively. Each spectrum is an average of 3 scans and has been corrected for buffer fluorescence acquired under the same conditions.

**RP-HPLC.** The oxidation state of the proteins was investigated using reverse-phase high-performance liquid chromatography (RP-HPLC). Each protein (50  $\mu\text{M}$  each) in 4 M GdnHCl, 50 mM Tris, pH 8.0, either with or without 500  $\mu\text{M}$  Tris(2-carboxyethyl) phosphine (TCEP) was injected onto an analytical RP C5 (15-cm by 4.6-mm) column and eluted using a gradient of water and acetonitrile at a flow rate of 1 ml/min (40% to 65% acetonitrile).

**Size exclusion chromatography.** The oligomeric state of the proteins was investigated using size exclusion chromatography. H1HA6\_PR8 and H1HA0HA6\_PR8 (200  $\mu\text{g}$  and 100  $\mu\text{g}$ , respectively), were loaded onto an analytical Superdex-200 (10- by 300-mm) column (GE Healthcare) at

concentrations of 1 mg/ml and 0.5 mg/ml in PBS (pH 7.4) at 25°C. The proteins were eluted in PBS (pH 7.4) at a flow rate of 0.5 ml/min, and the elution profiles were monitored by measuring the absorbance at 220 nm. Proteins used for calibration were thyroglobulin (669 kDa), ferritin (440 kDa),  $\beta$ -amylase (200 kDa), conalbumin (75 kDa), and RNase A (13.7 kDa).

**Animal immunization and challenge studies.** Female BALB/c mice (4 to 5 weeks old) were obtained from Charles River Laboratories (Wilmington, MA). Sets of 10 mice per immunogen were immunized intramuscularly with 20  $\mu\text{g}$  H1HA6\_PR8, 20  $\mu\text{g}$  H1HA0HA6\_PR8, 20  $\mu\text{g}$  H1HA6\_NC99, or 20  $\mu\text{g}$  H1HA6\_Cal09 along with 100  $\mu\text{g}$  CpG7909 adjuvant (TriLink BioTechnologies, San Diego, CA). Naïve mice and mice injected with adjuvant (100  $\mu\text{g}$  CpG7909) alone were used as controls. Mice immunized once intranasally with 0.1 90% lethal dose ( $\text{LD}_{90}$ ) of A/PR/8/34 acted as a positive control. The mice either were boosted with a repeat dose of the immunogens 4 weeks later (prime and boost groups) or were not boosted (prime only groups). Three weeks after the booster, the mice were intranasally challenged with 20  $\mu\text{l}$  of  $3.6 \times 10^7$  50% tissue culture infective dose ( $\text{TCID}_{50}$ )/ml ( $\sim 1 \text{LD}_{90}$ ) of homologous A/PR/8/34 virus. In order to test for protection against a higher dose of the virus, one group of mice that were primed and boosted with H1HA6\_PR8 were challenged with a 3  $\text{LD}_{90}$  dose of homologous PR8 virus. The body weight and survival of the mice were monitored for the next 20 days.

For evaluation of protection against viral replication in the lungs, mice were immunized with the prime-boost regimen as described above and challenged intranasally 3 weeks later with a sublethal dose of A/PR/8/34 (0.1  $\text{LD}_{90}$ ). Lungs were isolated at days 2, 4, 6, 8, and 10 postchallenge and used for determination of viral titers.

For generation of guinea pig antiserum, female guinea pigs (250 to 350 g; Charles River Laboratories) were immunized intramuscularly with 100  $\mu\text{g}$  of H1HA6 or H1HA0HA6 formulated with 250  $\mu\text{g}/\text{ml}$  CpG7909 (TriLink BioTechnologies) in 400  $\mu\text{l}$ . The immunizations were given three times at 4-week intervals. Blood samples were collected 3 weeks after each injection, and sera were stored at  $-70^\circ\text{C}$  until use. All animals were maintained in the animal facilities of Merck Research Laboratories in accordance with IACUC guidelines.

**Determination of anti-HA6 serum antibody titers.** HA6 proteins were immobilized on 96-well Nunc plates at 2  $\mu\text{g}$  per ml in 50  $\mu\text{l}$  PBS at 4°C overnight. Plates were washed six times with PBS containing 0.05% Tween 20 (PBST) and blocked with 3% skim milk in PBST. Sera were diluted starting at 1:100 and diluted in a 4-fold series in milk-PBST in a volume of 100  $\mu\text{l}$  per well. Plates were incubated for 2 h at room temperature followed by six washes with PBST. Horseradish peroxidase (HRP)-conjugated goat anti-mouse secondary antibody (Invitrogen) in milk-PBST (at 1:5,000 dilution) was added (50  $\mu\text{l}$  per well) and incubated at room temperature for 1 h. Plates were washed six times followed by addition of 100  $\mu\text{l}$  per well of the substrate 3,3',5,5'-tetramethylbenzidine (Virolabs, Inc.) and stopped after 3 to 5 min of development. The antibody titer was defined as the reciprocal of the highest dilution that gave an optical density at 450 nm ( $\text{OD}_{450}$ ) value above the mean plus 2 standard deviations.

**Determination of lung viral titers.** Mouse lung was homogenized in 3 ml Dulbecco's modified Eagle medium (Invitrogen, Grand Island, NY) containing 0.1% bovine serum albumin (Sigma-Aldrich Corp, St. Louis, MO) (DMEM-BSA). The virus titers were determined by plaque assay on Mardin-Darby canine kidney (MDCK) cells according to the method described in reference 17. Briefly, MDCK cells were cultured in 6-well plates in DMEM supplemented with 10% fetal bovine serum (HyClone, Logan, UT). Two hundred microliters of serially diluted test samples were added to each well of 6-well plates containing confluent MDCK cells. The plates were incubated at 37°C for 1 h. After the incubation, the samples were removed, and the cells were overlaid with 3 ml per well of 0.9% agar (BD Biosciences, San Jose, CA) in DMEM-BSA supplemented with 1  $\mu\text{g}/\text{ml}$  TPCK (tolylsulfonil phenylalanyl chloromethyl ketone)-treated trypsin (Sigma-Aldrich). After 4 days of incubation at 37°C and 5%  $\text{CO}_2$ , the agar

overlays were removed and the cells were fixed and stained with 10% glutaric dialdehyde (Sigma-Aldrich) and 0.67% crystal violet (Sigma-Aldrich) in water. Plaques were counted. All samples were tested in duplicates.

**Binding of antisera to recombinant HA proteins.** Binding of anti-H1HA6\_PR8 and anti-H1HA0HA6\_PR8 sera to various recombinant HA (rHA) proteins was measured using enzyme-linked immunosorbent assay (ELISA). Briefly, 250 ng of HA proteins from Protein Science Corp. (Viet/1203/04, New Caledonia/20/99, and pandemic H1N1 California/04/09) as well as H1HA6\_PR8 and H1HA0HA6\_PR8 proteins was immobilized on Nunc 96-well plates and blocked with 1% BSA in PBST (phosphate-buffered saline [pH 7.4] containing 0.5% Tween 20). Serial dilutions of sera (50  $\mu$ l) were added to the wells and incubated for 4 h. The plates were washed with PBST thrice and probed with alkaline phosphatase (ALP) conjugated anti-mouse Ab (1:10,000 diluted) for 2 h. After washing excess secondary Ab, the plates were developed by adding ALP substrate (*p*-nitrophenyl phosphate-alkaline phosphatase Yellow Liquid substrate from Sigma) and read in a plate reader at 405 nm after 1 h.

**Competition experiments with CR6261.** Sector Imager 6000 96-well plates (Meso Scale Discovery, Gaithersburg, MD) were coated with 50  $\mu$ l/well of 0.2  $\mu$ g/ml recombinant A/Vietnam/1203/2004 HA diluted in PBS. The plates were washed with PBST and blocked with 3% dry milk (LabScientific, Livingston, NJ) in PBST. Monoclonal antibody (MAb) CR6261 at 100 ng/ml was mixed with an equal volume of serial dilutions of the test guinea pig serum. To each well, 50  $\mu$ l of the mixture was added, and the plates were incubated at room temperature for 1 h. Plates were washed with PBST, and 100  $\mu$ l of Meso Scale Discovery Sulfo-tag-labeled goat anti-human IgG at 0.5  $\mu$ g/ml in PBST containing 3% dry milk per well was added and incubated at room temperature for 1 h, which was followed with an additional wash and addition of 150  $\mu$ l of Meso Scale Discovery read buffer T per well. The plates were read with Sector Imager 6000. All samples were run in duplicates. Percent competition was calculated as follows: % Competition =  $[(A - P)/A] \times 100$ , where *A* is the binding of CR6261 to HA in the absence of H1HA6 antiserum and *P* is the binding of CR6261 to HA in the presence of H1HA6 antiserum.

The luminescence signal from a Sector Imager was used as a measure of binding in the above equation.

**Sequence analysis of HA proteins from PR8, NC99, and Cal09 viruses.** To identify conserved regions in the HA stem of PR8, NC99, and Cal09 viruses, a sequence comparison was done. HA sequences of PR8 and NC99 or Cal09 were aligned using ClustalX, and residue-wise sequence identity was mapped onto the structure of HA (PDB ID 1ru7).

**Binding to broadly neutralizing antibody CR6261 by surface plasmon resonance (SPR).** CR6261 IgG (1,500 relative units [RU]) was immobilized onto a CM-5 Biacore Sensor chip surface using standard amine coupling, and binding of rHA A/Cal/07/2009 (Protein Science Corp.), H1HA6\_PR8, and H1HA0HA6\_PR8 to this MAb was recorded at 25°C on a Biacore 2000 optical biosensor (Biacore, Uppsala, Sweden). Proteins were passed over the sensor surface at a flow rate of 30  $\mu$ l/min in PBS (pH 7.4) containing 0.01% surfactant P20, and the association and dissociation were measured for 100 s and 200 s, respectively. The reported binding is subtracted for nonspecific binding to the control protein ovalbumin under the same conditions. The off-rates for H1HA6\_PR8 and H1HA0HA6\_PR8 were fitted in biphasic mode (double exponential decay) using the equation  $y = a_1 e^{(-k_1 \cdot t)} + a_2 e^{(-k_2 \cdot t)}$ , where *a*<sub>1</sub> and *a*<sub>2</sub> are the respective amplitudes and *k*<sub>1</sub> and *k*<sub>2</sub> are the respective dissociation constants of phase 1 and phase 2, *y* is the RU, and *t* is the time in seconds during the dissociation phase. The fractional amplitudes *fa*<sub>1</sub> and *fa*<sub>2</sub> are given by  $a_1/(a_1 + a_2)$  and  $a_2/(a_1 + a_2)$ , respectively. The off-rate for rHA was monophasic (*a*<sub>1</sub> = 0, *fa*<sub>2</sub> = 1). All analyte concentrations are given in trimer units, as the binding stoichiometry is 1 mol of HA trimer per immobilized CR6261 paratope.

## RESULTS AND DISCUSSION

**Design.** To design a stem-derived immunogen based on the sequence of the A/PR/8/34 virus from the H1N1 subtype, the accessibilities of all residues in the PR8 HA structure (PDB ID 1ru7) (11) were calculated, and HA1 fragments that interacted with HA2 were identified using the program PREDBURASA (16). The HA1 residue number 1 according to PDB 1ru7 numbering corresponds to residue number 14 in the full-length HA sequence with the signal peptide (sequence ID gi 194304803). Residues 1 to 160 of HA2 have been numbered from 501 to 660 in the PDB. We have used the PDB 1ru7 numbering when referring to residues in the constructs. The accessibilities of all residues in the HA1 chain in the presence and absence of the HA2 chain were calculated. HA1 residues that have a difference of 5 Å<sup>2</sup> or more in accessible surface area (ASA) in the above calculation and a 10% or higher accessibility difference were considered to be interacting with HA2. The list of interacting residues consisted of residues 5 to 14, 21 to 24, 32 to 36, 102 to 107, 265 to 268, 292 to 295, and 300 to 325 of HA1. Three fragments of HA were included in the immunogen: residues 501 to 672 of HA2 and residues 1 to 41 and 290 to 325 of HA1 (Fig. 1A). The fragments containing residues 102 to 107 and 265 to 268 of HA1 interact with the loop connecting the helices 4 and 5. Most of the interacting residues were polar ones, and these fragments were not included in the design. Next, accessibilities of all residues in the above fragments were calculated in the presence and absence of the rest of HA in order to identify residues that had become exposed in the fragments upon removal of the rest of HA. These residues were 41H, 290N, 298I, 299H, 301V, 303I, 304G, 305E, 306C, and 307P of HA1 and 564T, 566V, 568K, 569E, and 571N of HA2. Of these residues, the nonpolar residues that had a large change in ASA were mutated employing the program RosettaDesign (15), as increase in the exposed hydrophobic surface would be destabilizing for the protein. Exposure of polar residues on the surface is not expected to affect the stability of the protein.

At individual positions that were identified for mutation, all polar amino acid mutations were made using the RosettaDesign module. The structures and energies of the generated models were analyzed, and the best possible mutation for each position was chosen. For residues that were in close proximity in the structure, the calculations were repeated by mutating residues simultaneously at these positions. The mutations were chosen in a manner to ensure that there were no unfavorable electrostatic interactions because of their introduction. The final set of mutations was I298T, V301T, I303N, and C306S (in HA1) and V566T (in HA2).

In addition to the above mutations, in order to destabilize the low-pH conformation of HA, mutations F63D and L73D were introduced in the loop joining the helices 4 and 5 of HA2. As the low-pH structure is available only for HA from A/HK/68 (3), residues 51 to 103 of the PR/8/34 HA2 were modeled using this structure (PDB ID 1htm) as the template with the program Modeler (9, 24). The residues 63F and 73L are buried and are in close contact in the low-pH model, while they are exposed in the neutral-pH form (Fig. 1B and C). When Asp residues are introduced, the low-pH form should be destabilized, as formation of the low-pH trimeric structure would result in burial of charged Asp residues in the hydrophobic interior (residues 63 and 73 of HA2 are predicted to be at positions a and d of the extended coiled coil present in the low-pH structure).

Constructs H1HA6\_PR8 and H1HA0HA6\_PR8 were based on

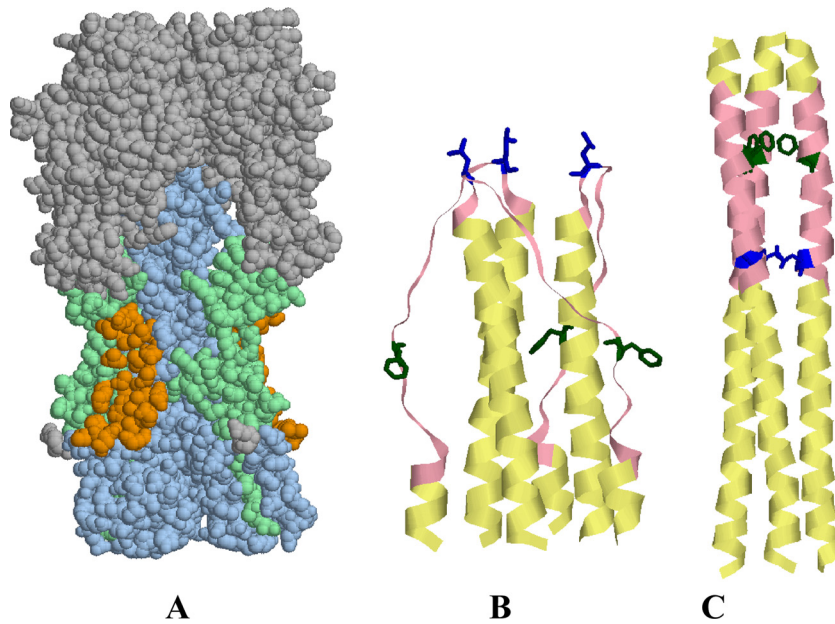


**FIG 1** Structures of the A/PR/8/34 HA ectodomain (A) and HA2 fragment residues 51 to 103 at neutral pH (B) and low pH (C). (A) The colored regions are fragments included in the H1HA6 design (HA2 chains are shown in blue and HA1 in green). The globular head domain that is not part of H1HA6 is shown in gray. The residues constituting the epitope for the broadly neutralizing antibody CR6261 are a part of H1HA6 (the epitope is in orange). (B and C) Residues 57 to 75 of HA2 are shown in pink. These residues form the loop between helices 4 and 5 at neutral pH and form a part of the extended coiled coil at low pH. Residues 63F (green) and 73L (blue) of HA2 are exposed in the neutral pH conformation, while they are buried in the trimeric core of the coiled coil at low pH. The neutral-pH structure (B) has been taken from the full-length neutral-pH structure of PR8/34 HA (PDB ID 1ru7). This region corresponds to residues 551 to 603 of the HA2 chains in this PDB. The low-pH model (C) has been generated by homology modeling using the program Modeller. The images were generated using Rasmol (21).

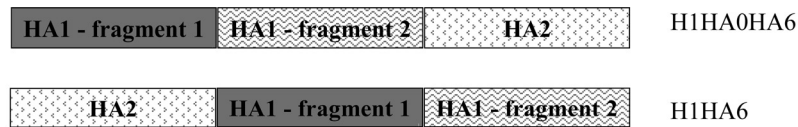
the A/PR/8/34 HA sequence (sequence ID gi 194304803) taken from the influenza virus resource at NCBI (1). The three chosen fragments were connected by flexible linkers in two ways. The length of the linkers was decided based on the C $\alpha$ -C $\alpha$  distances between the residues to be connected in the crystal structure (PDB ID 1ru7), and the sequence consisted of repeats of the tripeptide GSA. These linkers have been used previously by us in other protein designs (33), are expected to be soluble and flexible, and should not disrupt the structure of the fragments they link.

The construct H1HA0HA6\_PR8 was made by connecting the C terminus of the second HA1 fragment (residues 290 to 325) with the N terminus of HA2 using the natural linker sequence (residues 326 to 330) present in HA0. The cleavage site residue 330R was mutated to Q in order to abolish trypsin cleavage. A mutation of cleavage site residue to Q at the cleavage site of HK/68 HA was previously shown to result in an uncleavable precursor of HA (4). This molecule did not undergo the low-pH conformational change even upon exposure to low pH. It has been shown that cleavage of the precursor to HA1 and HA2 fragments and dissociation of the HA1 domain fragment is essential for the low-pH conformational change and viral pathogenicity (13). H1HA0HA6\_PR8 has residues 3 to 41 of HA1, a 3-amino-acid linker (GSA), residues 290 to 330 of HA1 with cleavage site residue 330R changed to Q (to abolish trypsin cleavage), and residues 501 to 660 of HA2.

In the construct H1HA0HA6, the fusion peptide is expected to be exposed (by comparison with the precursor HA0 structures of HK/68 [PDB ID 1ha0]). However, the conformation of this region is different in the 1918 H1N1 HA0 (PDB ID 1rd8) and the cleavage site loop abuts the HA surface (28). In order to avoid problems

that might arise due to the exposure of the hydrophobic fusion peptide, the circular permutant H1HA6\_PR8 was made. This construct contains the same fragments as H1HA0HA6\_PR8 joined together with linkers in a different manner (Fig. 2). The HA2 subunit has been placed at the N terminus of this molecule. The fusion peptide would therefore be buried when the molecule folds into the desired neutral-pH conformation and is expected to more closely mimic the stem region of the native trimer. The construct H1HA6\_PR8 has residues 501 to 672 of HA2, a 6-amino-acid linker (GSAGSA), residues 1 to 41 of HA1, and a 3-amino-acid linker (GSA), followed by residues 290 to 325 of HA1. In the crystal structure of the PR/8/34 HA (PDB ID 1ru7) residues beyond 660 of HA2 are disordered. Hence, the residues to be connected and linker length for the H1HA6\_PR8 construct were decided based on the HK/68 HA structure (PDB ID 1hgd).

In order to test for the ability of HA stem immunogens to elicit cross-protection against multiple strains of viruses, immunogens based on the sequences of two H1N1 viruses with different degrees of HA sequence identity to A/PR/8/34 were designed. The alternative approach of immunizing with H1HA6\_PR8 and carrying out a heterologous challenge with seasonal or pandemic H1N1 was not attempted because of lack of availability of appropriate mouse-adapted challenge strains other than A/PR/8/34. Stem domain immunogens similar to H1HA6\_PR8 were made from HA proteins of these viruses. The design of H1HA6\_NC99 was based on the sequence of A/New Caledonia/20/99 HA (sequence ID gi 9849784), which has an identity of 88% with PR8 HA. The design of H1HA6\_Cal09 was based on A/Cal/07/09 HA (sequence ID gi 227831808), which has an identity of 82% with PR8 HA. Residues corresponding to those in H1HA6\_PR8 were chosen for the de-



1) *MGSSHHHHHSSGLVPRGSHMDADTICIGYHANNSTDTVDTVLEKNVTVTHSVNLLLED SHGSA<sup>NS</sup>SSLPYQ NTHPTTNGESPKYVRS AKLRMVTGLRNIPSIQSQGLFGAIA GFIEGGWTGMIDGWYGYHHQNEQGSYAA DQKSTQNAINGITNKVNTVIEKMNIQDTATGKEFNKDEKRMENLNKKVDDGFLDIWYTNAELLVLENER TLDHFDSNVKNLYEKVKSQ LKNNAKEIGNGCFEFYHKCDNECMESVRNGTYDYP*

2) *MGLFGAIA GFIEGGWTGMIDGWYGYHHQNEQGSYAADQKSTQNAINGITNKVNTVIEKMNIQDTATG KEFNKDEKRMENLNKKVDDGFLDIWYTNAELLVLENER TLDHFDSNVKNLYEKVKSQ LKNNAKEIGNG CFEFYHKCDNECMESVRNGTYDYPKYSEESKLNREKGSAGSAAADADTICIGYHANNSTDTVDTVLEKNV TVTHSVNLLLED SHGSA<sup>NS</sup>SSLPYQNTHTPTTNGESPKYVRS AKLRMVTGLRNIPKLA<sup>AA</sup>LEHHHHHHH*

3) *MGLFGAIA GFIEGGWTGMVDGWYGYHHQNEQGSYAADQKSTQNAINGITNKVNSVIEKMNTQDTAT GKEFNKDEKRMENLNKKVDDGFLDIWYTNAELLVLENER TLDHFDSNVKNLYEKVKSQ LKNNAKEIGN GCFEFYHKCDNECMESVRNGTYDYPKYSEESKLNREKGSAGSAATYADTICIGYHANNSTDTVDTVLEKN VTVTHSVNLLLED SHGSA<sup>NS</sup>SSLPFQNTHTPTTNGQSPKYVRS AKLRMVTGLRNIPKLA<sup>AA</sup>LEHHHHHHH*

4) *MGLFGAIA GFIEGGWTGMVDGWYGYHHQNEQGSYAADLKSTQNAIDEITNKVNSVIEKMNTQDTAV GKEFNKDEKRIENLNKKVDDGFLDIWYTNAELLVLENER TLDYHDSNVKNLYEKVRSQ LKNNAKEIGN GCFEFYHKCDNTCMESVRNGTYDYPKYSEEAKLNREEGSAGSATANADTLCIGYHANNSTDTVDTVLEKN VTVTHSVNLLLEDKHSANTSLPFQNTHTPTTNGKSPKYVKSTKLRLATGLRNIPKLA<sup>AA</sup>LEHHHHHHH*

**FIG 2** Connectivity and sequences of the designed constructs. H1HA0HA6 consists of residues 3 to 41 of HA1, a 3-amino-acid linker (GSA), residues 290 to 330 of HA1 with cleavage site residue 330R changed to Q (to abolish trypsin cleavage), and residues 501 to 660 of HA2. The circular permutant H1HA6 design consists of residues 501 to 672 of HA2, a 6-amino-acid linker (GSAGSA), residues 1 to 41 of HA1, and a 3-amino-acid linker (GSA) followed by residues 290 to 325 of HA1. Mutations were incorporated into the constructs to stabilize the neutral pH conformation (in bold) and to remove exposed hydrophobic patches. The sequences of H1HA0HA6\_PR8 (1), H1HA6\_PR8 (2), H1HA6\_NC99 (3), and H1HA6\_Cal09 (4) are given. Mutated residues are underlined, and linkers and vector-derived sequences are shown in italics. The numbering scheme is the same as in the PDB ID 1ru7. The box diagrams above the sequences show the way in which the HA fragments have been connected. The lengths of the fragments are not to scale.

sign. The mutations that were introduced in H1HA6\_PR8 to remove hydrophobic patches and to destabilize the low-pH form were introduced in these constructs. Additionally, residue 305E (HA1) was mutated to Q (in H1HA6\_NC99) or K (in H1HA6\_Cal09) to prevent repulsion with 563D of HA2. Residue 566V (HA2) was not changed in H1HA6\_Cal09, as this residue was buried and packed with other residues in its vicinity (PDB ID 3l3g) (37).

The final sequences of the designed proteins (after incorporation of mutations to destabilize the low-pH structure and to increase solubility) are given in Fig. 2. The H1HA6 design is very similar to the one described earlier for an H3N2 HA (2). However, the design H1HA0HA6 has not been tested before. A headless HA construct from A/PR/8/34 (expressed in 293T cells incorporated into virus-like particles [VLPs]) described earlier has a connectivity similar to that of H1HA0HA6 (27).

#### Expression, purification, and biophysical characterization.

The proteins H1HA6\_PR8, H1HA0HA6\_PR8, H1HA6\_NC99, and H1HA6\_Cal09 were expressed in *E. coli* under the control of the T7 promoter and purified from inclusion bodies by Ni-affinity chromatography under denaturing conditions. The proteins were refolded by dialysis against water. The yield was 2 to 3 mg/liter for each of the proteins. Far-UV CD spectra of the purified proteins indicated that they were well folded and were largely helical (Fig. 3A). A shift in the emission maxima of the intrinsic fluorescence of the proteins from 345 nm to 357 nm upon denaturation indicated that the proteins were well folded and compact under native conditions (Fig. 3B). Mass spectrometric analysis of H1HA6\_PR8 revealed that there were two species: the full-length protein and the N-terminal Met-cleaved form. The observed masses correspond to the fully oxidized forms in both species with

a deficit of 4 Da compared to the reduced protein. This corresponds to the formation of two disulfide bonds (expected masses, 30,258.3 Da for the N-terminal Met-cleaved protein and 30,389.4 Da for the full-length protein; observed masses, 30,258.3 Da and 30,385.4 Da, respectively).

Reverse-phase HPLC studies indicated that the proteins H1HA6\_PR8 and H1HA0HA6\_PR8 were oxidized and the native disulfide bonds are formed as is expected in properly folded HA (Fig. 3C). Oxidized H1HA6\_PR8 eluted primarily as a single peak on the reverse-phase HPLC. Upon reduction, the peak eluted at higher acetonitrile. This is expected because reduction should lead to greater exposure of the hydrophobic surface. H1HA0HA6\_PR8 was partially aggregated because of intermolecular disulfide bonds and showed two major peaks in the oxidized state. The aggregates were removed upon reduction with the reducing agent TCEP. The crystal structure of HK/68 HA in the HA0 precursor form revealed that the highly hydrophobic fusion peptide was exposed and the cleavage site at the junction of the HA1 and HA2 was accessible (4). This resulted in a surface cavity in the HA0 molecule that is otherwise filled with the fusion peptide in the postcleavage neutral-pH form (35). In the H1HA0HA6\_PR8 design, the HA1 and HA2 fragments have been connected using the natural linker present in the HA mimicking the HA0 form.

The apparent molecular weight and oligomeric state of H1HA6\_PR8 and H1HA0HA6\_PR8 were assessed by analytical size exclusion chromatography (Fig. 4) experiments. The data indicated that H1HA6\_PR8 is likely to be largely trimeric in solution, whereas a substantial proportion of H1HA0HA6 forms higher-molecular-weight aggregates. The higher aggregation propensity of H1HA0HA6\_PR8 relative to H1HA6\_PR8 is probably due to the exposed hydrophobic fusion peptide and the cavity

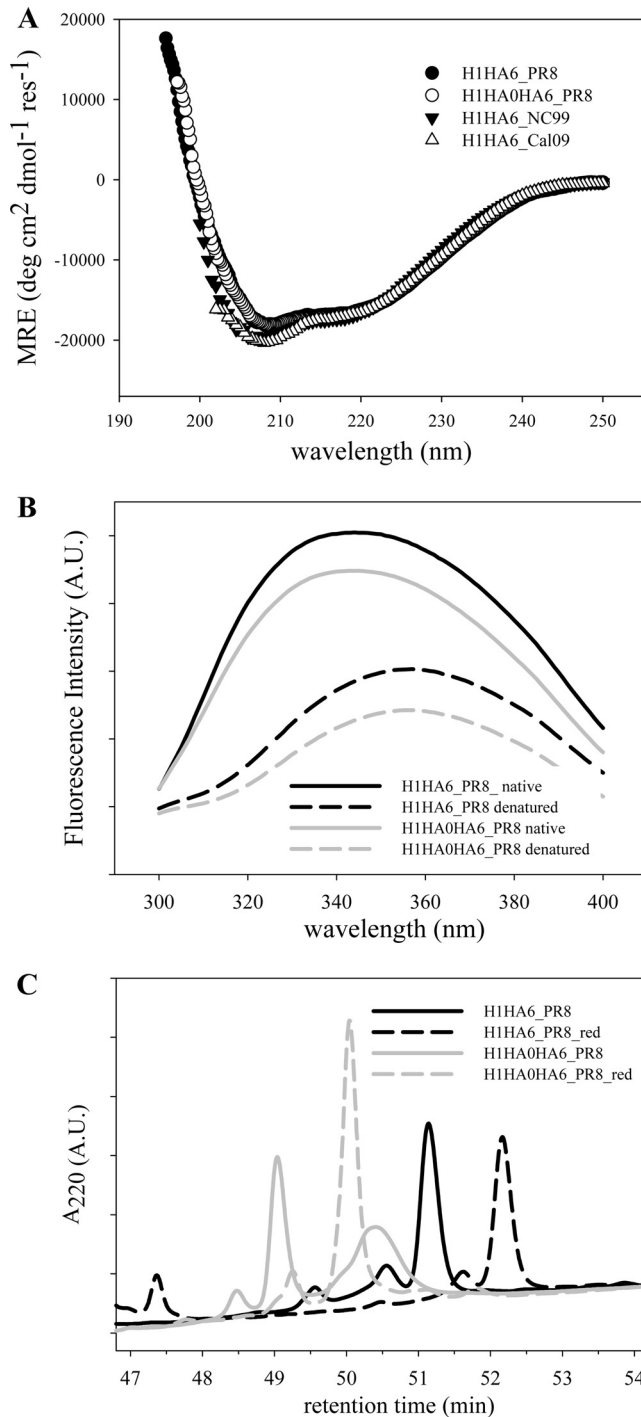


**FIG 3** Biophysical characterization of the designed stem domain immunogens. (A) Far-UV CD spectra of H1HA6\_PR8, H1HA0HA6\_PR8, H1HA6\_NC99, and H1HA6\_Cal09 (5  $\mu$ M each) in PBS, pH 7.4, at 25°C. (B) Fluorescence emission spectra of 2  $\mu$ M H1HA6\_PR8 (black) and H1HA0HA6\_PR8 (gray) under native conditions (20 mM Tris, pH 8.0) (solid line) or denaturing conditions (6 M GdnHCl, 20 mM Tris, pH 8.0) (dashed line) at 25°C. Excitation was at 280 nm. (C) Reverse-phase HPLC profiles of H1HA6\_PR8 (in black) and H1HA0HA6\_PR8 (in gray). The reduced proteins (dashed lines) have retention times that are different from those of the native proteins (solid lines), indicating that the proteins are oxidized. H1HA6\_PR8 shows a single major oxidized peak in the native form, while H1HA0HA6\_PR8 is partially aggregated because of intermolecular disulfide bonds.

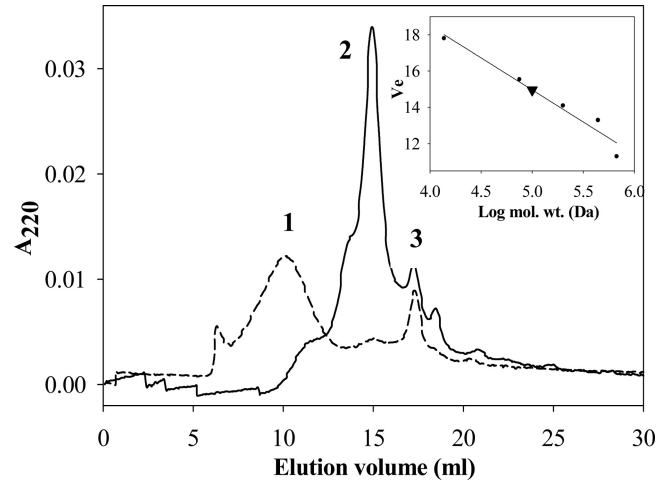


**FIG 4** Gel filtration profile of H1HA6\_PR8 (solid line) and H1HA0HA6\_PR8 (dotted line) on a Superdex 200 analytical column in PBS, pH 7.4, at 25°C. The inset shows the column calibration curve. A large fraction of the H1HA6\_PR8 elutes at a volume that corresponds to its trimeric mass (peak 2, inverted triangle in insert). However, a major fraction of H1HA0HA6\_PR8 is aggregated and elutes close to the void volume (peak 1), while a small fraction elutes at a volume that corresponds to its monomeric mass (peak 3). The expected trimeric mass of H1HA6\_PR8 is 91.2 kDa, and the estimated mass for peak 2 from the calibration curve is around 90 kDa. The expected monomeric mass of H1HA0HA6\_PR8 is 29.5 kDa.

described above. The circularly permuted H1HA6\_PR8 design seems to be better than the H1HA0HA6\_PR8 design for the above reason.

**Immunization and challenge.** Details of the immunization schedule and survival after challenge are presented in [Table 1](#). H1HA0HA6\_PR8 and H1HA6\_PR8 were used to immunize BALB/c mice, and both constructs were highly immunogenic as inferred from the postdose 2 (PD2) titers ([Fig. 5A](#) and [B](#)). At week 7, 3 weeks after the second immunization, mice were challenged with 1 LD<sub>90</sub> of A/PR/8/34 virus. The mice lost weight initially after the challenge but later recovered completely ([Fig. 6B](#)). Both immunogens successfully protected mice from homologous viral challenge ([Fig. 6A](#)), though the extent of weight loss was slightly less for mice immunized with H1HA6. Immunization with H1HA6\_PR8 also provided significant protection against a higher dose of the virus (3 LD<sub>90</sub>) ([Fig. 6A](#)). As a positive control, one group was intranasally immunized with 0.1 LD<sub>90</sub> of A/PR/8/34 virus.

Immunization with stem domain immunogens from drifted viruses H1HA6\_NC99 and H1HA6\_Cal09 also protected mice from lethal challenge by A/PR/8/34 virus ([Fig. 6A](#)). This indicates that stem domain immunogens are capable of protecting against several strains of viruses within the subtype, unlike conventional vaccines that are ineffective against drifted viruses. However, mice immunized with a single dose of H1HA6 immunogens succumbed to infection ([Table 1](#)). Immune responses generated by a single-dose immunization are probably insufficient for protection.

We have previously shown ([Table S1](#) in the supplemental material in reference [2](#)) that in all H1 strains the exposed residues in the stem domain (H1HA6) are 90% conserved. In general, HA proteins have >80% sequence identity in the entire HA within a subtype ([14](#), [19](#), [22](#)). Cal09 is one of the most divergent of the

TABLE 1 Immunization dose regimen used for challenge studies

Group	Vaccine antigen/adjuvant (time of immunization)	% Survival <sup>a</sup>	Log <sub>10</sub> anti-HA6 titer <sup>b</sup>
1	20 µg H1HA0HA6_PR8/100 µg CpG7909 (wk 0 and wk 4)	100	ND <sup>c</sup>
2	20 µg H1HA6_PR8/100 µg CpG7909 (wk 0 and wk 4)	100	5.0
3	20 µg H1HA6_NC99/100 µg CpG7909 (wk 0 and wk 4)	90	4.5
4	20 µg H1HA6_Cal09/100 µg CpG7909 (wk 0 and wk 4)	90	4.1
5	20 µg H1HA6_PR8/100 µg CpG7909 (wk 0 only)	20	3.6
6	20 µg H1HA6_NC99/100 µg CpG7909 (wk 0 only)	10	3.0
7	20 µg H1HA6_Cal09/100 µg CpG7909 (wk 0 only)	30	3.3
8	20 µg H1HA6_PR8/100 µg CpG7909 (wk 0 and wk 4) <sup>d</sup>	70	4.6
9	PR8 virus, 0.1 LD <sub>90</sub> , intranasal (wk 0 only)	100	ND
10	100 µg CpG7909 (wk 0 and wk 4)	30	ND
11	None	20	ND

<sup>a</sup> Each group consisted of 10 BALB/c mice. Mice were challenged with 1 LD<sub>90</sub> of A/PR/8/34 virus at week 7. The survival of the mice after viral challenge was monitored for 20 days postchallenge.

<sup>b</sup> Antibody titers of sera collected at week 6 (after dose 2) against recombinant HA (A/PR/8/34) were measured by ELISA.

<sup>c</sup> ND, not determined.

<sup>d</sup> Mice in this group were challenged with 3 LD<sub>90</sub> of A/PR/8/34 virus at week 7.

H1N1 strains compared to PR8 (the sequence identity between HA proteins of these strains is 82%). An HA6 immunogen designed from Cal09 HA protected against lethal challenge with PR8 virus. Therefore, we expect an H1HA6 vaccine to protect against the vast majority of H1 strains. In contrast, successive vaccine strains have a sequence identity as high as 98% in the entire HA, i.e., a 2% sequence variation in HA is sufficient to reduce the efficacy of a conventional flu vaccine.

**Lung viral titers.** To further evaluate the effect of vaccine on viral replication, two groups of mice were immunized either with H1HA6\_PR8 plus CpG7909 adjuvant or with the adjuvant alone. Three weeks after the second immunization, mice were challenged intranasally with a sublethal dose of PR8 (0.1 LD<sub>90</sub>). Five mice from each group were sacrificed at days 2, 4, 6, 8, and 10 postchallenge, and the viral titers in the lungs were determined. Whereas no difference between the two groups was observed at days 2 and 4, the vaccine group showed 1.5-log-lower titers ( $3 \times 10^3$  PFU/ml versus  $6.7 \times 10^4$  PFU/ml;  $P < 0.05$ ) at day 6, and it had no detectable virus at day 8, when 4 of 5 mice in the control group still had detectable virus. The data indicate that immunization with H1HA6 was able to reduce lung viral replication.

**Binding of antisera to HA proteins of various strains.** ELISA studies were carried out to examine binding of antisera from animals immunized with H1HA6\_PR8, H1HA0HA6\_PR8, and intranasal PR8 virus with HA proteins from various strains. H1HA6\_PR8 and H1HA0HA6\_PR8 were highly immunogenic, and antisera of immunized mice had titers of  $10^6$  against homologous antigens (Fig. 5A and B). Sera from mice immunized intranasally with 0.1 LD<sub>90</sub> of PR8 virus had 100-fold-lower titers

against H1HA6\_PR8 and H1HA0HA6\_PR8 (Fig. 5C). The HA1 subunit of the HA protein forms an exposed globular head domain that contains the receptor binding site. Most antibodies induced by natural viral infection are directed against this domain (35). The lower anti-H1HA6\_PR8 titers (reflective of anti-HA2 titers) in animals immunized with whole PR8 virus are consistent with this observation.

Anti-H1HA6\_PR8 sera reacted strongly with recombinant HA proteins from all other strains tested (Fig. 5A; Table 2). The titers are consistent with the sequence identity of these proteins and A/PR/8/34 HA (NC/99 [identity in HA1, 83%, and in HA2, 96%]

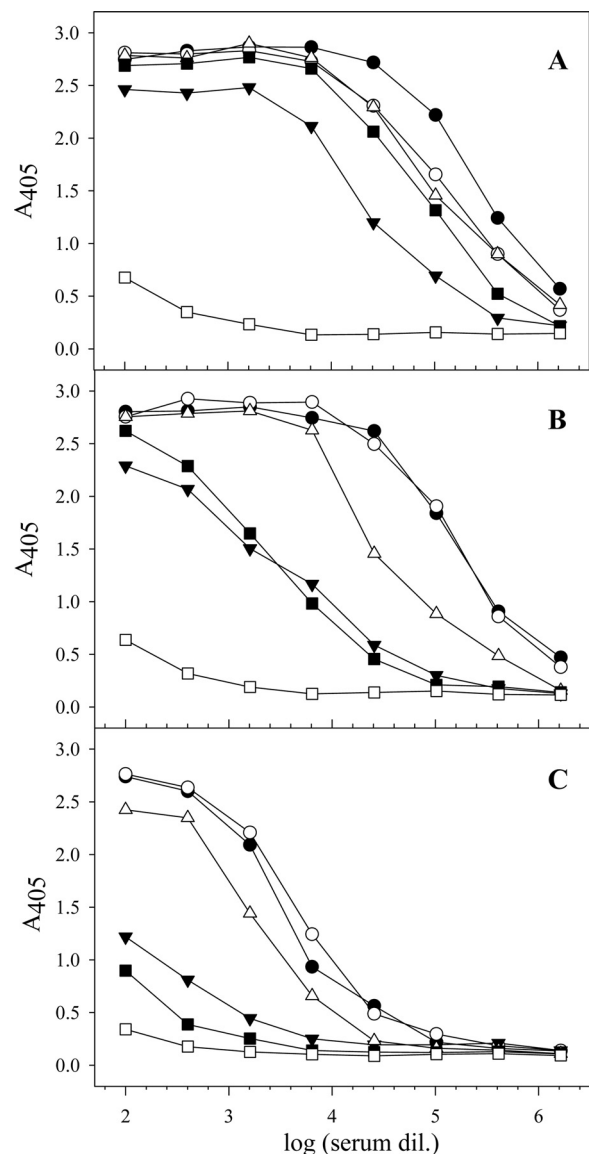
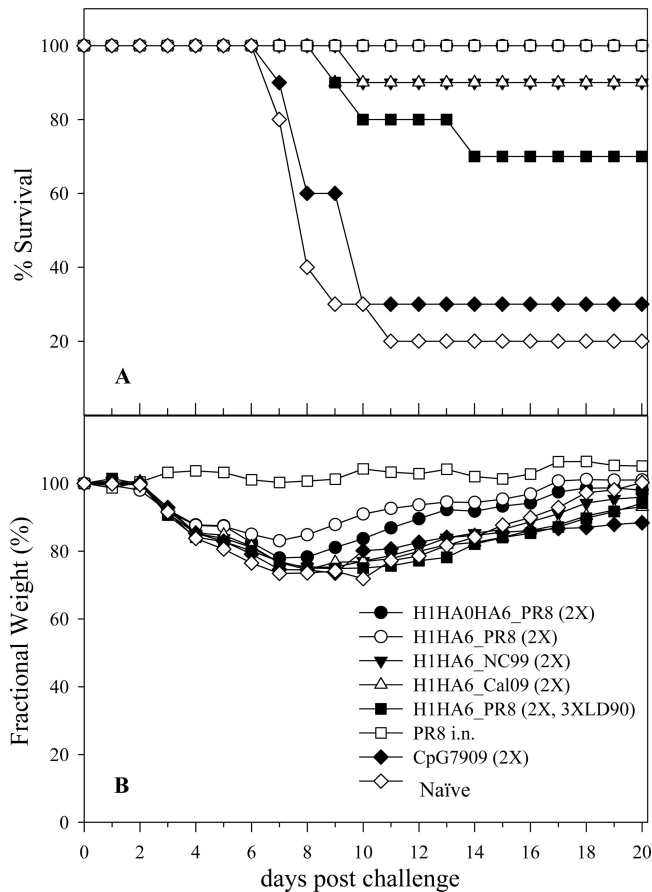


FIG 5 Anti-HA titers in sera from H1HA6\_PR8, H1HA0HA6\_PR8, and PR8 virus-immunized mice. ELISA titers of anti-H1HA6\_PR8 sera (A), anti-H1HA0HA6\_PR8 sera (B), and virus-immunized sera (anti-PR8, administered intranasally) (C) against H1HA6 (●), H1HA0HA6 (○), rHA H5N1 Vietnam/1203/04 (Viet/04) (▼), rHA H1N1 New Caledonia/20/99 (NC/99) (△), rHA pandemic H1N1 California/4/09 (Cal/09) (■), and negative control (ovalbumin) (□). Cross-reactive titers decrease in the following order: anti-H1HA6\_PR8 sera > anti-H1HA0HA6\_PR8 sera > anti-PR8 sera.



**FIG 6** Survival and weight loss studies in mice immunized with H1HA6 and H1HA0HA6 immunogens. (A) Percent survival after challenge with a lethal dose of A/PR/8/34 virus; (B) fractional weight (%) of the surviving mice. Mice immunized twice with H1HA6\_PR8 and H1HA0HA6\_PR8 were completely protected against the homologous virus challenge (1 LD<sub>90</sub>). Prime boost immunization with H1HA6\_PR8 also protected against a higher dose of the virus (3 LD<sub>90</sub> [3XLD90]). HA stem domain immunogens from two other H1N1 viruses provided cross-protection against PR8 challenge (1 LD<sub>90</sub>), showing that stem domain immunogens can provide broad-range protection.

> pandemic strain Cal/09 [identity in HA1, 74.7%, and in HA2, 92%] > Viet/04 [identity in HA1, 4.7%, and in HA2, 79.7%]). Anti-H1HA0HA6\_PR8 sera had measurably lower cross-reactive titers than H1HA6\_PR8 sera (Fig. 5B). RP-HPLC and gel filtration profiles of H1HA0HA6\_PR8 showed that the protein is aggregated. Lower cross-reactive titers in animals immunized with this protein are observed, probably because of its aggregation-prone nature. In animals immunized with PR8 virus, the cross-reactive titers are ~100-fold less than in H1HA6\_PR8-immunized animals (Fig. 5C). While H1HA6\_PR8 elicited high titers of antibody

reactive against HA from both pandemic H1N1 and avian H5N1, immunization with PR8 virus failed to elicit such antibodies. Thus, by directing the immune response to the HA2 domain of the protein, higher cross-reactive titers are achieved. Computational redesigning and trimming of immunodominant epitopes have been successfully used to focus immune responses to conserved epitopes and identify broadly neutralizing Abs in other highly variable viral proteins like HIV envelope (6, 36).

**Competition experiments with broadly neutralizing antibody CR6261.** Antisera from H1HA6-immunized mice were tested in a standard microneutralization assay as described previously (2). H1HA6 antisera did not show neutralization in this assay (data not shown). The 50% inhibitory concentration (IC<sub>50</sub>) for CR6261 measured by us using this assay was 11.69 μg/ml. Earlier studies with an H3HA-derived HA6 protein (from the HK/68 virus) in FcRγ knockout (KO) mice indicated that protection conferred by anti-HA6 antibodies is largely mediated by antibody-dependent effector functions such as antibody-dependent cell-mediated cytotoxicity (ADCC), although competition studies indicated that neutralizing 12D1-like antibodies were also likely to contribute to the observed protection (2). In the present case also, such effector functions are likely to contribute to the observed protection.

Since the microneutralization assay is not very sensitive in detecting stem-directed neutralizing antibodies, the presence of antibodies to a known stem epitope (targeted by the broadly neutralizing antibody CR6261) was tested in a competition binding experiment. Because of lack of sufficient supply of the mouse serum, the competition assay was carried out with sera from immunized guinea pigs. Anti-H1HA6\_PR8 sera and anti-H1HA0HA6\_PR8 sera were able to compete with CR6261 for binding to recombinant Viet/04 HA (Fig. 7), indicating that CR6261-like antibodies were elicited by immunization with stem-derived immunogens. However, naïve sera and sera from animals immunized with an HK/68 H3HA-derived stem immunogen (2) did not show significant competition. Stem-directed neutralizing antibodies like CR6261 mediate neutralization by inhibition of viral and host membrane fusion, unlike head-directed antibodies, which have hemagglutinin inhibition (HAI) activity and inhibit viral binding to receptors on the host cells. The lack of neutralization observed with H1HA6 sera suggests that the CR6261-like Abs must be present at levels lower than the 11.69 μg/ml IC<sub>50</sub> value for CR6261.

**Binding of H1HA6 proteins to broadly neutralizing Ab CR6261.** The binding of the designed immunogens to a broadly neutralizing antibody, CR6261, was tested by SPR (Table 3 and Fig. 8). Recombinant CR6261 was produced based on the published sequence (32) in 293T cells. Recombinant HA from A/Cal/07/09 bound the Ab with *K<sub>d</sub>* (dissociation constant) of 6 nM, which is similar to the value of 3.2 nM reported previously (31).

**TABLE 2** Half maximal cross-reactive ELISA titers of anti-HA6 sera against HA of different strains

Antigen	% Identity with A/PR/8/34 HA			Log <sub>10</sub> (half-maximal ELISA titers)		
	HA1	HA2	HA6	Anti-H1HA6 sera	Anti-H1HA0HA6 sera	Anti-PR8 virus sera
Seasonal H1N1 New Caledonia/20/99	83	96	95	5.3	4.6	3.4
Pandemic H1N1 California/07/2009	75	92	90	5.0	3.7	2.6
H5N1 Vietnam/1203/2004	55	80	76	4.4	3.7	3.0

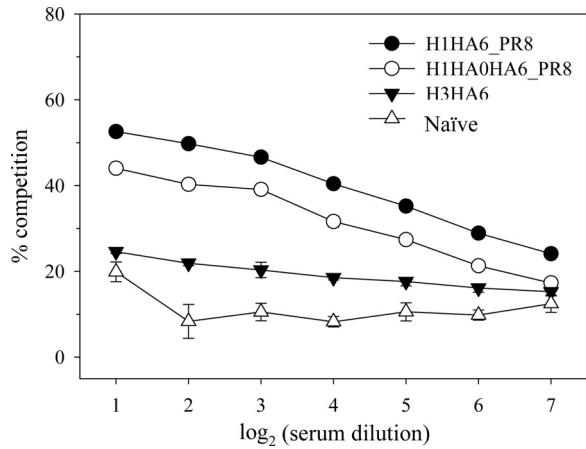


**FIG 7** Competition of HA6 antisera with CR6261. Antisera from guinea pigs immunized with stem immunogens (H1HA6\_PR8, H1HA0HA6\_PR8, or H3HA6\_HK68) were tested for competition binding to recombinant Viet/04 HA in the presence of 50 ng/ml of CR6261. Compared to naïve sera and sera from animals immunized with an H3HA-derived stem immunogen (H3HA6\_HK68), H1HA6\_PR8 antisera and H1HA0HA6\_PR8 antisera showed greater competition with CR6261.

H1HA6\_PR8 and H1HA0HA6\_PR8 also bound CR6261, albeit with lesser affinity (Fig. 8B and C). The dissociation rates for both H1HA6\_PR8 and H1HA06\_PR8 were found to be biphasic, in contrast to rHA, which was monophasic. The relative amplitudes of the fast and slow phases were approximately 0.15 and 0.85, respectively, for both proteins. The gel filtration data (Fig. 4) suggest that H1HA6\_PR8 is largely trimeric while H1HA0HA6\_PR8 is largely aggregated. It is likely that the biphasic dissociation rates are due to heterogeneity in sample aggregation state. The relative amplitudes suggest that slow dissociation results from trimer and higher-order aggregates in the cases of H1HA6\_PR8 and H1HA0HA6\_PR8, respectively. The fast dissociation likely results from monomeric species in both cases.

Although H1HA6\_PR8 protein is a trimer and H1HA0HA6\_PR8 is a higher-order aggregate, we have indicated analyte concentrations in trimer units in order to compare apparent  $K_d$  values. The binding stoichiometry known from the cocrystal structure of CR6261 with HA is one monomer of the HA trimer per paratope; however, when the analyte binds to CR6261 IgG that is immobilized on the SPR chip, we anticipate that one molecule of the analyte will bind at a single immobilized paratope.

**Sequence analysis.** To identify conserved regions in the stem of PR8, NC99, and Cal09 HAs, a pairwise sequence comparison was done. Residue-wise conservation was mapped onto the crystal structure. Figure 9 shows several regions on the stem that are conserved. Identical residues are in red, and nonidentical residues

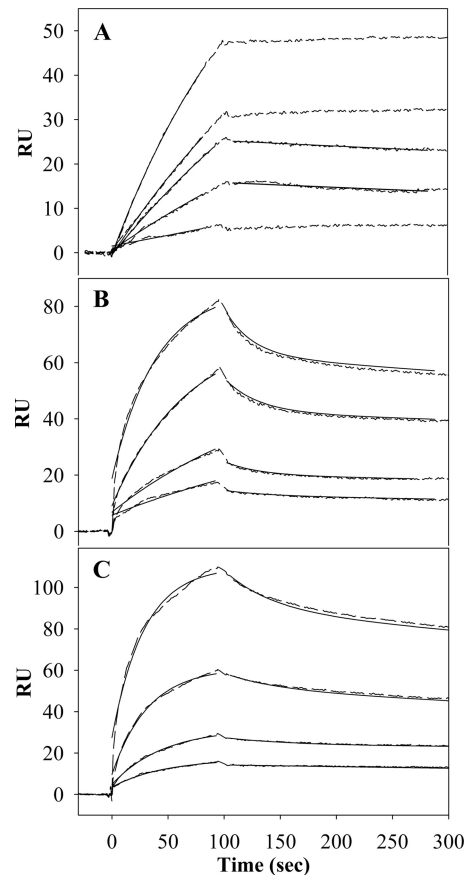


**FIG 8** Binding of rHA A/California/09, H1HA6\_PR8, and H1HA0HA6\_PR8 to the broadly neutralizing Ab CR6261. Biacore sensorgram overlays of the binding of 0.33 nM, 3.33 nM, 16.67 nM, 33.3 nM, and 66.67 nM rHA California/09 (A); 1.33  $\mu$ M, 2.67  $\mu$ M, 5.33  $\mu$ M, and 10.67  $\mu$ M H1HA6\_PR8 (B); and 1.33  $\mu$ M, 2.67  $\mu$ M, 5.33  $\mu$ M, and 10.67  $\mu$ M H1HA0HA6\_PR8 (C) at 25°C in PBS (pH 7.4) containing 0.01% surfactant P20. Sensorgram overlays are shown as dotted lines, and the corresponding fits are shown as solid lines. The kinetic parameters for binding are given in Table 3. In all cases, analyte concentration increases from the bottom to the top curve.

are in blue. The conserved regions are likely targets for cross-reactive antibodies that provide protection against PR8 challenge. The highly conserved CR6261 epitope is one such epitope on the stalk (Fig. 1A) that could mediate protection against several strains and subtypes of flu viruses.

Several broadly neutralizing antibodies that bind to conserved stem epitopes have been isolated recently (8, 21, 30, 31, 34). Some of them bind to viruses of the H3 clade (mAb 12D1), while others bind to HA from the H1 clade. Three neutralizing Abs that bind to

**TABLE 3** Kinetic parameters<sup>a</sup> for binding of recombinant HA A/California/07/09, H1HA6\_PR8, and H1HA0HA6\_PR8 to immobilized CR6261 as determined by SPR

Analyte	$k_{on}$ ( $M^{-1} s^{-1}$ )	$k_{off1}$ ( $s^{-1}$ )	$k_{off2}$ ( $s^{-1}$ )	fa1	fa2	$K_D1$ ( $\mu$ M)	$K_D2$ ( $\mu$ M)
rHA A/Cal/07/09	$(1.37 \pm 0.6) \times 10^5$		$(8.7 \pm 4.7) \times 10^{-4}$		1.0		$0.006 \pm 0.0008$
H1HA6_PR8	$(2.1 \pm 0.4) \times 10^3$	$(3.9 \pm 0.8) \times 10^{-2}$	$(5.3 \pm 1.5) \times 10^{-4}$	$0.18 \pm 0.04$	$0.82 \pm 0.04$	$19.2 \pm 2.7$	$0.26 \pm 0.1$
H1HA0HA6_PR8	$(1.9 \pm 0.9) \times 10^3$	$(1.7 \pm 0.2) \times 10^{-2}$	$(4.0 \pm 1.7) \times 10^{-4}$	$0.13 \pm 0.02$	$0.87 \pm 0.02$	$9.0 \pm 2.6$	$0.19 \pm 0.07$

<sup>a</sup>  $k_{on}$  is the rate constant for association. The rate constants for dissociation of H1HA6\_PR8 and H1HA0HA6\_PR8 are both biphasic;  $k_{off1}$  and  $k_{off2}$  are the rate constants for dissociation, while fa1 and fa2 are the corresponding fractional amplitudes for phase 1 and phase 2, respectively.  $K_D$  is the equilibrium dissociation constant. Data are representative of two independent trials.

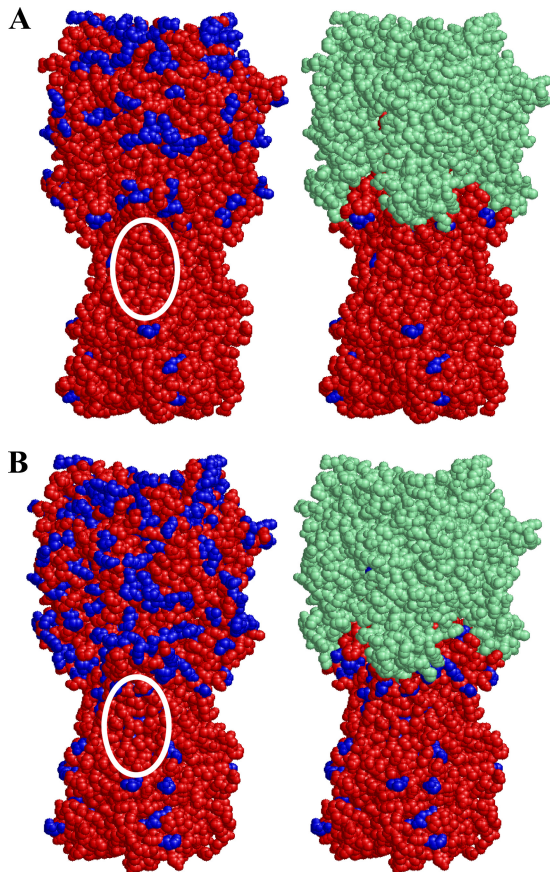


**FIG 9** Sequence conservation between the HA proteins of PR8, NC99 (A), and PR8, Cal09 (B) viruses. Residue-wise sequence conservation was mapped onto the HA crystal structure (PDB ID 1ru7) shown in spacefill representation. Identical residues are in red, and nonidentical residues are in blue. The CR6261 epitope is circled in white. The head domain of HA, which is not a part of the design of H1HA6, is in pale green on the right of each panel to highlight conserved regions in the stem domain constructs.

A/Albany/20/1957 (H2)  
 A/Vietnam/1203/2004 (H5)  
 A/Puerto Rico/8/1934 (H1)  
 A/duck/Guangxi/038/2009 (H6)  
 A/gull/Alaska/2009 (H13)  
 A/gull/Alaska/2009 (H16)  
 A/duck/Thailand/2009 (H11)  
 A/mallard/Minnesota/2008 (H8)  
 A/turnstone/Delaware/2008 (H12)  
 A/Vietnam/2010 (H9)  
 A/duck/Korea/2005 (H4)  
 A/mallard/Astrakhan/1982 (H14)  
 A/Hong Kong/1968 (H3)  
 A/New York/107/2003 (H7)  
 A/duck/Australia/341/1983 (H15)  
 A/duck/South Africa/2009 (H10)

	a		d		a		d												
E	K	M	N	T	Q	E	F	E	A	M	G	K	E	F	S	N	L	E	R
D	K	M	N	T	Q	E	F	E	A	M	G	R	E	F	N	N	L	E	R
E	K	M	N	I	Q	E	F	T	A	M	G	K	E	F	N	K	L	E	K
D	K	M	N	T	Q	E	F	E	A	M	G	H	E	F	S	N	L	E	R
D	K	M	N	G	N	Y	D	S	I	R	G	E	F	N	Q	V	E	K	
E	K	M	N	G	N	Y	D	S	I	R	G	E	F	N	Q	V	E	K	
D	R	M	N	T	N	F	E	S	V	Q	H	E	F	S	E	I	E	E	
D	K	M	N	R	E	F	E	V	V	N	H	E	F	S	E	V	E	K	
D	K	M	N	K	Q	E	D	V	M	N	H	E	F	S	E	V	E	S	
D	K	M	N	K	Q	E	I	I	D	H	E	F	S	E	I	E	A		
E	K	T	N	E	K	Y	H	Q	I	E	K	E	F	E	Q	V	E	G	
E	K	T	N	E	K	Y	H	Q	I	E	K	E	F	E	Q	V	E	G	
E	K	T	N	E	K	F	H	Q	I	E	K	E	F	S	E	V	E	G	
G	K	T	N	Q	F	E	L	I	D	N	E	F	N	E	I	E	Q		
E	K	T	N	T	Q	F	E	L	I	D	N	E	F	T	E	V	E	Q	
E	K	T	N	T	E	F	E	S	E	S	E	F	S	E	I	E	H		
						63					66					70			73

**FIG 10** Sequence alignment of HA2 residues 57 to 75 from representative strains of the 16 different influenza A HA subtypes. Sequences have been taken from the influenza virus resource at NCBI and numbered with the first residue of HA2 as residue 1 (1). Marked in the boxes are residues that are predicted to be buried in the trimeric interface of the coiled coil at low pH: residues 63, 66, 70, and 73 of HA2, which would be at positions a, d, a, and d of the helical wheel, respectively. These residues are in a relatively exposed loop in the neutral-pH structure. Hence, introduction of Asp residues at these positions would not affect the neutral pH structure of the stem-derived immunogens. However, the low-pH conformation would be greatly destabilized owing to the unfavorable burial of the charged Asp residues in the hydrophobic core of the coiled coil.

that are expected to be exposed in the neutral-pH structure of the stem-derived immunogens but buried in the low-pH structure of HA. As can be seen, in all cases such residues exist, and it is therefore feasible to design similar immunogens for any subtype of influenza A virus by mutating one or more of these residues. Such immunogens may find application in future pandemics.

We have so far shown that it is possible to design stem-derived immunogens for the seasonal H3N2 (2) and H1N1 (present study) subtypes of the virus that confer protection against homologous challenge. Given the high similarity between the HA6 regions of the seasonal and pandemic H1N1, the high cross-reactivity of H1N1 elicited sera with pandemic H1N1 HA, the ability of H1HA6\_Cal09 to protect against PR8 challenge, and the presence of CR6261-like antibodies in the polyclonal sera, it is likely that the H1HA6\_PR8 immunogen would confer protection against pandemic H1N1 viruses and other H1 viruses.

## ACKNOWLEDGMENT

We acknowledge the Council of Scientific and Industrial Research for financial support.

## REFERENCES

- Bao Y, et al. 2008. The influenza virus resource at the National Center for Biotechnology Information. *J. Virol.* 82:596–601.
- Bommakanti G, et al. 2010. Design of an HA2-based *Escherichia coli* expressed influenza immunogen that protects mice from pathogenic challenge. *Proc. Natl. Acad. Sci. U. S. A.* 107:13701–13706.
- Bullough PA, Hughson FM, Skehel JJ, Wiley DC. 1994. Structure of influenza haemagglutinin at the pH of membrane fusion. *Nature* 371:37–43.
- Chen J, et al. 1998. Structure of the hemagglutinin precursor cleavage site, a determinant of influenza pathogenicity and the origin of the labile conformation. *Cell* 95:409–417.
- Chen J, et al. 1995. A soluble domain of the membrane-anchoring chain of influenza virus hemagglutinin (HA2) folds in *Escherichia coli* into the low-pH-induced conformation. *Proc. Natl. Acad. Sci. U. S. A.* 92:12205–12209.
- Correia BE, et al. 2011. Computational protein design using flexible backbone remodeling and resurfacing: case studies in structure-based antigen design. *J. Mol. Biol.* 405:284–297.
- Corti D, et al. 2011. A neutralizing antibody selected from plasma cells that binds to group 1 and group 2 influenza A hemagglutinins. *Science* 333:850–856.
- Ekiert DC, et al. 2009. Antibody recognition of a highly conserved influenza virus epitope. *Science* 324:246–251.
- Eswar N, et al. 2006. Comparative protein structure modeling using Modeller. *Curr. Protoc. Bioinformatics Chapter 5:Unit 5.6.* doi:10.1002/0471250953.bi0506s15.
- Fouchier RA, et al. 2005. Characterization of a novel influenza A virus hemagglutinin subtype (H16) obtained from black-headed gulls. *J. Virol.* 79:2814–2822.
- Gambliin SJ, et al. 2004. The structure and receptor binding properties of the 1918 influenza hemagglutinin. *Science* 303:1838–1842.
- Gerhard W. 2001. The role of the antibody response in influenza virus infection. *Curr. Top. Microbiol. Immunol.* 260:171–190.
- Godley L, et al. 1992. Introduction of intersubunit disulfide bonds in the membrane-distal region of the influenza hemagglutinin abolishes membrane fusion activity. *Cell* 68:635–645.
- Kawaoka Y, Yamnikova S, Chambers TM, Lvov DK, Webster RG. 1990. Molecular characterization of a new hemagglutinin, subtype H14, of influenza A virus. *Virology* 179:759–767.
- Kuhlman B, et al. 2003. Design of a novel globular protein fold with atomic-level accuracy. *Science* 302:1364–1368.
- Lee B, Richards FM. 1971. The interpretation of protein structures: estimation of static accessibility. *J. Mol. Biol.* 55:379–400.
- Matrosovich M, Matrosovich T, Garten W, Klenk HD. 2006. New low-viscosity overlay medium for viral plaque assays. *Virology* 343:63.
- Myers JK, Pace CN, Scholtz JM. 1997. Helix propensities are identical in proteins and peptides. *Biochemistry* 36:10923–10929.
- Nobusawa E, et al. 1991. Comparison of complete amino acid sequences and receptor-binding properties among 13 serotypes of hemagglutinins of influenza A viruses. *Virology* 182:475–485.
- Okuno Y, Isegawa Y, Sasao F, Ueda S. 1993. A common neutralizing epitope conserved between the hemagglutinins of influenza A virus H1 and H2 strains. *J. Virol.* 67:2552–2558.
- Okuno Y, Matsumoto K, Isegawa Y, Ueda S. 1994. Protection against the mouse-adapted A/FM/1/47 strain of influenza A virus in mice by a monoclonal antibody with cross-neutralizing activity among H1 and H2 strains. *J. Virol.* 68:517–520.
- Rohm C, Zhou N, Suss J, Mackenzie J, Webster RG. 1996. Characterization of a novel influenza hemagglutinin, H15: criteria for determination of influenza A subtypes. *Virology* 217:508–516.
- Russell RJ, et al. 2004. H1 and H7 influenza haemagglutinin structures extend a structural classification of haemagglutinin subtypes. *Virology* 325:287–296.
- Sali A, Blundell TL. 1993. Comparative protein modelling by satisfaction of spatial restraints. *J. Mol. Biol.* 234:779–815.
- Skehel JJ, Wiley DC. 2000. Receptor binding and membrane fusion in virus entry: the influenza hemagglutinin. *Annu. Rev. Biochem.* 69:531–569.
- Smirnov YA, Lipatov AS, Gitelman AK, Claas EC, Osterhaus AD. 2000. Prevention and treatment of bronchopneumonia in mice caused by mouse-adapted variant of avian H5N2 influenza A virus using monoclonal antibody against conserved epitope in the HA stem region. *Arch. Virol.* 145:1733–1741.
- Steel J, et al. 2010. Influenza virus vaccine based on the conserved hemagglutinin stalk domain. *mBio* 1(1):e00018–10. doi:10.1128/mBio.00018-10.
- Stevens J, et al. 2004. Structure of the uncleaved human H1 hemagglutinin from the extinct 1918 influenza virus. *Science* 303:1866–1870.
- Stropkovska A, et al. 2009. Broadly cross-reactive monoclonal antibodies against HA2 glycopeptide of influenza A virus hemagglutinin of H3 subtype reduce replication of influenza A viruses of human and avian origin. *Acta Virol.* 53:15–20.
- Sui J, et al. 2009. Structural and functional bases for broad-spectrum neutralization of avian and human influenza A viruses. *Nat. Struct. Mol. Biol.* 16:265–273.
- Throsby M, et al. 2008. Heterosubtypic neutralizing monoclonal antibodies cross-protective against H5N1 and H1N1 recovered from human IgM+ memory B cells. *PLoS One* 3:e3942. doi:10.1371/journal.pone.0003942.
- van den Brink E, de Kruif CA, Throsby M. 2007. Human binding molecules capable of neutralizing influenza virus H5N1 and uses thereof. International patent application no. PCT/EP2007/059356.
- Varadarajan R, et al. 2005. Characterization of gp120 and its single-chain derivatives, gp120-CD4D12 and gp120-M9: implications for targeting the CD4i epitope in human immunodeficiency virus vaccine design. *J. Virol.* 79:1713–1723.
- Wang TT, et al. Broadly protective monoclonal antibodies against H3 influenza viruses following sequential immunization with different hemagglutinins. *PLoS Pathog.* 6:e1000796. doi:10.1371/journal.ppat.1000796.
- Wilson IA, Skehel JJ, Wiley DC. 1981. Structure of the haemagglutinin membrane glycoprotein of influenza virus at 3 Å resolution. *Nature* 289:366–373.
- Wu X, et al. 2010. Rational design of envelope identifies broadly neutralizing human monoclonal antibodies to HIV-1. *Science* 329:856–861.
- Xu R, et al. 2010. Structural basis of preexisting immunity to the 2009 H1N1 pandemic influenza virus. *Science* 328:357–360.